Eur Biophys J (1991) 19:203–211

European Biophysics Journal

Monte-Carlo-simulations of voltage fluctuations in biological membranes in the case of small numbers of transport units

B. Kleutsch and E. Frehland

Institut für Biologie, Universität Konstanz, Postfach 5560, W-7750 Konstanz, Federal Republic of Germany

Received May 24, 1990/Accepted in revised form November 20, 1990

Abstract. Some years ago a theory of non-equilibrium voltage fluctuations in biological membranes was developed (Frehland and Solleder 1985, 1986) under a linearisation condition which is valid for a great number of transport units. In order to get an insight into the stochastic behaviour of such systems, consisting of small numbers of transport units, we carried out Monte-Carlo-simulations and compared the mean voltage course and the spectral density with the results of the previous theory. Under parameter conditions of biological relevance no significant differences from the behaviour of systems with large numbers, as predicted from the earlier theory, could be found in the case of rigid pores and ion carriers. However, in the case of small numbers, channels with open-closed-kinetics showed great deviations. With increasing number of transport units agreement with the previous theory was obtained.

Key words: Voltage fluctuations – Ion channels – Carrier – Non-equilibrium – Poisson-process

1. Introduction

Experiments and theoretical treatments on electric noise in biological membranes are usually concerned with the analysis of current noise under constant voltage or of voltage noise under current-clamp conditions. A general theoretical approach to transport fluctuations permits the calculation of current noise spectra (Frehland 1978, 1982). However, voltage fluctuations are of special interest because they set a limit to the transduction of signals at nerve excitation. The voltage noise amplitude has to be smaller than the signal to be detected.

A recently developed theory of voltage noise (Frehland and Solleder 1985, 1986; Solleder and Frehland 1986; Frehland 1988) based on a Master equation approach (van Vliet and Fassett 1965) is constrained to several conditions. Generally the validity of linearisation conditions requires that the number of transport units must be large. However, in modern experimental methods the condition of large numbers is not always satisfied; on the contrary, often only single-channel-measurements are made.

Up to now, no theoretical approach to these small number systems was available. From other systems, e.g. growing populations, it is known that the stochastic behaviour at small numbers can be completely different from that obtained by approximation procedures for solving the Master equation (Dubin 1976).

In this situation it is of great theoretical and experimental interest to get more insight into the effects of small numbers in stochastic membrane transport systems on the membrane voltage behaviour.

Monte-Carlo-simulations of voltage fluctuations for small numbers of transport units (Kleutsch 1988) are presented here and the results compared with the earlier theory (Frehland and Solleder 1985, 1986; Solleder and Frehland 1986). For special transport systems great differences are obtained, which disappear with increasing numbers.

2. Monte-Carlo-simulation of voltage fluctuations

2.1. *Rigid pores with one binding site*

Using a simple example, the case of a rigid pore with one binding site is discussed first (Fig. 1). Current fluctuations of pores with one binding site have been discussed by Läuger (1975). The voltage fluctuations of a great number of pores has been handled by Frehland and Solleder (1985, 1986). We have done Monte-Carlo-simulation of voltage fluctuations for a small number of transport units.

The "single-file" assumption requires that the binding site may only be occupied by one ion as a consequence of ionic interactions (Frehland and Stephan 1979). Because of the current-clamp condition, a constant net flux charge is delivered to one side of the membrane and drained from

Offprint requests to: B. Kleutsch

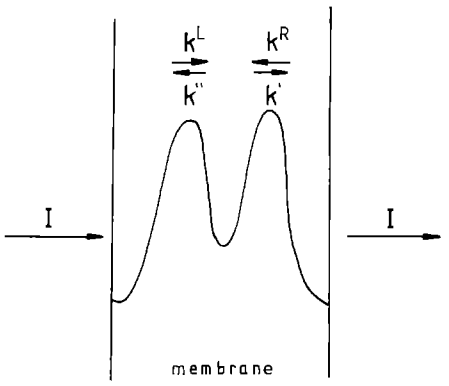

Fig. 1. Two barrier model for pores with one binding

the other side. It is further assumed that the current-clamp causes a change of voltage, which is continuous in time. This would lead to a linear increase of the voltage if there were no jumps of ions across the membrane, i.e. if the potential barriers were infinitely large. In the case of finite barriers, transition of an ion with charge q across the membrane with capacitance C causes a voltage change of

$$\Delta U = \pm \frac{q}{C}. \tag{1}$$

The sign is positive if the directions of jump and current-clamp are the same. If the binding site is occupied or becomes empty, the voltage is changed by

$$\Delta U = \pm \frac{\gamma_i}{C}, \quad i=1, 2. \tag{2}$$

γ_1 and γ_2 describe the degree of symmetry of the pore. Restriction to the symmetrical case then yields

$$\gamma_1 = \gamma_2 = \frac{q}{2}. \tag{3}$$

A change of voltage will influence the transition frequencies (k_B: Boltzmann factor, T: Temperature) according to the rate theory (Eyring 1935; Zwolinsky et al. 1949)

$$\begin{aligned} k^L(U) &= k_0^L \exp\left(+\gamma_1 \frac{U-U_0}{2k_B T}\right) \\ k^R(U) &= k_0^R \exp\left(-\gamma_2 \frac{U-U_0}{2k_B T}\right) \\ k'(U) &= k_0' \exp\left(+\gamma_2 \frac{U-U_0}{2k_B T}\right) \\ k''(U) &= k_0'' \exp\left(-\gamma_1 \frac{U-U_0}{2k_B T}\right) \end{aligned} \tag{4}$$

with

$$\begin{aligned} k_0^L &= k^L(U_0) \\ k_0^R &= k^R(U_0) \\ k_0' &= k'(U_0) \\ k_0'' &= k''(U_0). \end{aligned} \tag{5}$$

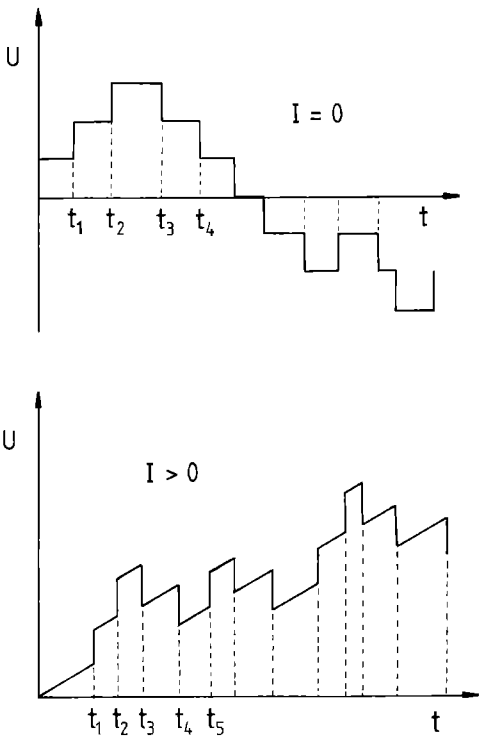

Fig. 2. Model of voltage fluctuations under equilibrium ($I=0$) and non-equilibrium conditions ($I>0$)

2.2. *Two methods for Monte-Carlo-simulation*

We distinguish between two possibilities of Monte-Carlo-simulation. First, the time axis is divided into equal intervals. In each interval, uniformly distributed random numbers decide if a transition occurs or not. However, to get a good approximation, the time intervals chosen must be sufficiently short. In order to save computer-calculating-time we have selected a second method, where an event will occur in every iteration step. In contrast to the first method, the time intervals are not equal because the times of transitions are directly calculated.

2.2.1. Equilibrium. We begin with the equilibrium case, where current and average voltage are zero. Voltage changes are caused by the ionic jumps. Voltage as a function of time remains constant between two jump events (Fig. 2). Hence the rate frequencies remain constant between two transitions, and on each segment the process can be regarded as Poisson-distributed. The probability density on the segment i for an allowed jump with frequency $k(t_i)$ is given by

$$w(t) = k(t_i) \exp(-k(t_i)(t-t_i)), \quad t \in (t_i, t_{i+1}). \tag{6}$$

Uniformly distributed random numbers $z \in (0, 1)$ are generated by the algorithm of Kirkpatrick and Stoll (1981). To yield random numbers $t \in (t_i, \infty)$, which are distributed with the probability density of (6), the uniformly distributed random numbers $z \in (0, 1)$ can be transformed (Sobol 1971) by

$$\int_{t_i}^{t_{i+1}} w(t')\,dt' = z. \tag{7}$$

Then from (6) and (7) the time of the next event

$$t_{i+1} = -\frac{1}{k(t_i)} \ln(1-z) + t_i \,. \tag{8}$$

If more than one possible transition exists, the time for each possible event has to be calculated. The transition with the shortest time is chosen. Before the next step the frequencies, k_i, have to be recalculated because the voltage has been changed by the previous transition event.

2.2.2. Non-equilibrium. Simulation in the non-equilibrium case is different to that for the equilibrium case because the assumption of a Poisson-process in each time segment is no longer valid. Because the assumption of a continuous current clamp means a linear increase of the voltage (Fig. 2), rate frequencies are continuously changing between two transitions. In order to obtain the generalization for (8), the probability distribution function $p(t)$ has to be calculated.

If the time interval Δt is very small, then

$$(1-p(t))\, k(t)\, \Delta t$$

is the probability that no event will occur until time t but will occur in the interval $(t,\ t+\Delta t)$. Then the following differential equation may be constructed

$$\frac{\mathrm{d}p(t)}{\mathrm{d}t} = (1-p(t))\, k(t) \,. \tag{9}$$

The voltage in the i-th time interval

$$U(t) = U(t_i) + \frac{I}{C}(t-t_i) \quad \text{with} \quad t_i \le t < t_{i+1} \tag{10}$$

determines the rate frequencies

$$k(t) = k_0 \exp\left(\frac{\pm\gamma_{1,2}}{2k_B\, T}\left(U(t_i) + \frac{I}{C}(t-t_i)\right)\right). \tag{11}$$

Substitution for $k(t)$ in (9) and solution of the differential equation yields

$$p(t) = 1 - \exp\left(-\frac{k(t_i)}{\alpha}(\exp(\alpha(t-t_i)) - 1)\right) \tag{12}$$

with

$$\alpha := \frac{\pm\gamma_{1,2}}{2k_B\, T} \cdot \frac{I}{C} \,. \tag{13}$$

The probability distribution function $p(t)$ at time t_{i+1} can be written as

$$p(t_{i+1}) = \int_{t_i}^{t_{i+1}} w(x)\, \mathrm{d}x = z \,. \tag{14}$$

Equations (14) and (12) yield

$$t_{i+1} = -\frac{1}{\alpha} \ln\left(1 - \frac{\alpha}{k(t_i)} \ln(1-z)\right) + t_i \,. \tag{15}$$

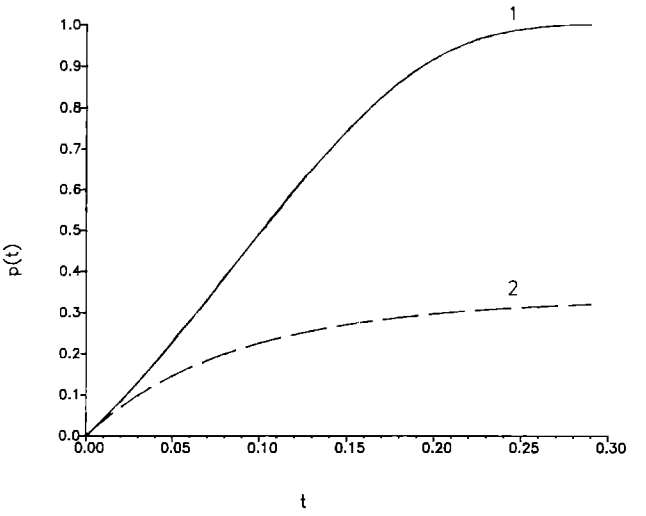

Fig. 3. Probability distribution function of the non-Poisson-process under non-equilibrium conditions for a jump of an ion in the same (*1*) and in the opposite (*2*) direction to the current. k_B, T, q, C, $I=1$, $\gamma_{1,2}=0.5$, $k^L(0)$, $k^R(0)$, $k'(0)$, $k''(0)=4$

The simulation is then done in the same way as described for the equilibrium case. But in the non-equilibrium case (15) does not deliver for every random number z a finite value for t (see Fig. 3). The probability distribution function for a jump in the opposite direction ($\alpha<0$) to the current does not have the limit 1 for $t=\infty$. That means, that in contrast to the equilibrium case, there is a finite probability that a jump will never occur.

3. Numerical calculation of the spectral density

The spectral density $G(\omega)$ of a quantity $U(t)$ (voltage) can be calculated by Fourier transformation of the autocorrelation function $R(s)$ or the covariance functions $C(s)$. This relation is given by Wiener (1930; Khintchine 1934):

$$G(\omega) = 4 \int_0^\infty C(s) \cos(\omega\, s)\, \mathrm{d}s \tag{16}$$

with

$$\omega = 2 \cdot \pi \cdot f \,. \tag{17}$$

The autocorrelation function is defined as

$$R(s) = \lim_{T\to\infty} \frac{1}{T} \int_0^T U(t)\, U(t+s)\, \mathrm{d}t \tag{18}$$

and the covariance function as the difference

$$C(s) = R(s) - \langle U \rangle^2 \,. \tag{19}$$

$\langle U \rangle$ denotes the expectation value (ensemble average) of U. Because the stochastic process is ergodic (Frehland 1982), the ensemble average can be replaced by the time average.

The numerical calculation of $R(s)$ uses an approximation of the integral (18) by

$$R(t_k) = \frac{1}{m} \sum_{i=1}^{m} U(t_i)\, U(t_{i+k}) \,. \tag{20}$$

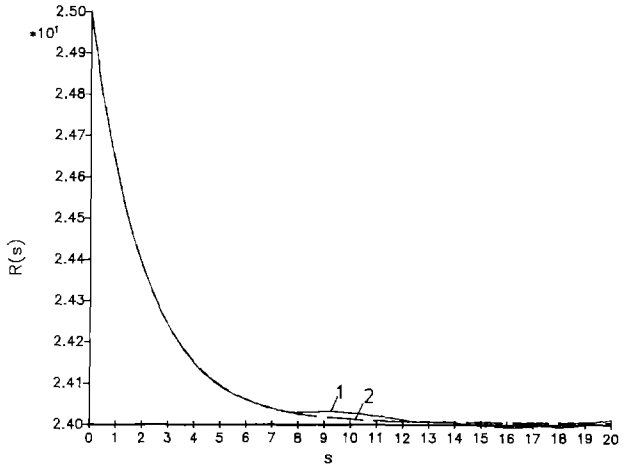

Fig. 4. Autocorrelation function for a single-file-pore with one binding site: (*1*) Monte-Carlo-simulation, (*2*) fitted function. $k^L(0)$, $k^R(0)$, $k'(0)$, $k''(0)$, C, k_B, T, q, $N_{P'}=1$, $m=5\cdot 10^4$, $\gamma_{1,2}=0.5$, $I=1.6$

Figure 4 shows an autocorrelation function calculated by Monte-Carlo-simulation for one pore with one binding site and single-file condition. The second curve is a fitted function of the form

$$R(s)\approx a\cdot\exp\left(-\frac{s}{b}\right)-c \tag{21}$$

with the parameters a, b and c. The covariance function corresponding to the fitted function is then given by

$$C(s)=a\cdot\exp\left(-\frac{s}{b}\right) \tag{22}$$

because $c=R(\infty)=\langle U\rangle^2$ (Bendat and Piersol 1971).

The spectral density G can be calculated with the use of the Wiener-Khintchine-relation (16):

$$G(\omega)=\frac{4ab}{1+\omega^2 b^2}. \tag{23}$$

In other examples treated in the following sections it is necessary to fit the autocorrelation function by a Gauß function or by a sum of two exponential or Gauß curves.

4. Numerical results

4.1. Single-file-channel with one binding site

In the equilibrium case, the voltage fluctuations of single-file-pores with one binding site can be represented by a resistance R and a capacitance C in a parallel circuit (DeFelice 1981):

$$G(\omega)=\frac{4\sigma^2 RC}{1+\omega^2(RC)^2} \tag{24}$$

with

$$\sigma^2=\frac{k_B T}{C}. \tag{25}$$

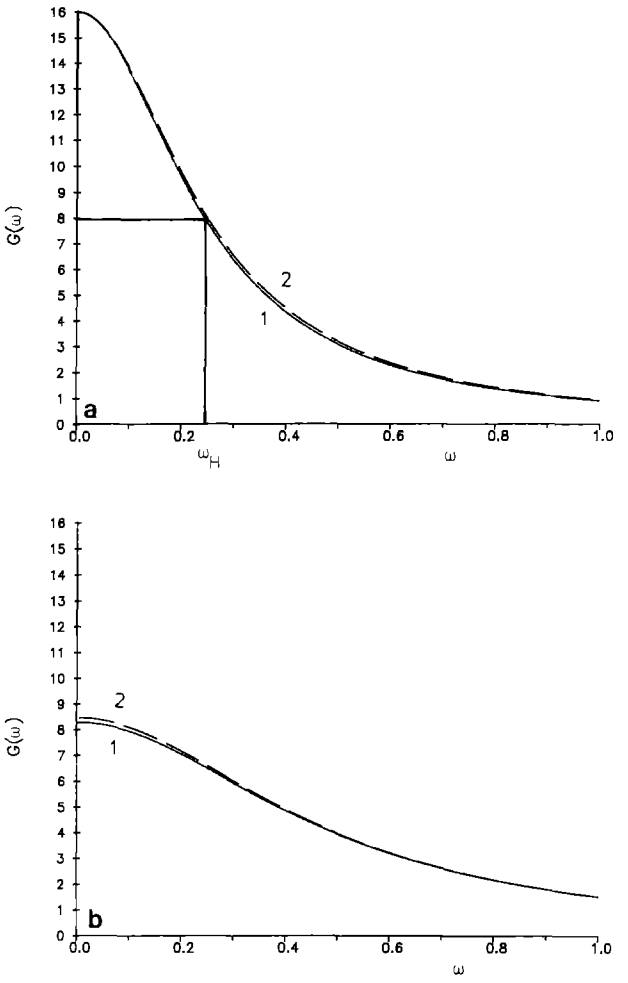

Fig. 5. a Spectral density for a single-file-pore with one binding site at equilibrium: (*1*) Monte-Carlo-simulation, (*2*) corresponding RC-circuit (24). $k^L(0)$, $k^R(0)$, $k'(0)$, $k''(0)$, C, k_B, T, q, $N_{P'}=1$, $\gamma_{1,2}=0.5$, $I=0$. **b** Spectral density for a single-file-pore with one binding site at equilibrium: (*1*) Monte-Carlo-simulation, (*2*) theory of Frehland and Solleder (1985, 1986). Parameters as in **a** except $I=1.6$

Under the condition of a linear voltage-current relation, which is valid for a small current, the resistance of a membrane with N_P identical pores can be calculated as follows.

$$R=\frac{4k_B T}{q^2 N_p k_0}. \tag{26}$$

It is further assumed that all rate frequencies have the same value, k_0, at equilibrium. According to Fig. 5 a, the spectra of the simulation and of the corresponding RC-circuit agree within the accuracy of the calculation. We have done many further simulations with different numbers of channels, different capacitances and resistances, always getting good agreement with (24).

In the non-equilibrium case, (24) is no longer valid. Frehland and Solleder (1986) developed a general theory for the calculation of the spectral density of voltage fluctuations which can be applied for different transport systems. However, this theory is based on a linearisation which can be assumed to be valid only in the limit of large numbers of transport units. Nevertheless, comparisons of

this theory with our simulations for low numbers did not show significant differences for the channel model considered (Fig. 5b).

4.2. *Carrier-mediated ion transport*

An alternative basic concept of membrane transport is the concept of carrier mediated ion transport. For example, valinomycin-mediated transport through lipid bilayers has been extensively investigated (Stark et al. 1971; Läuger and Stark 1970; Knoll and Stark 1975). It is assumed that single carrier molecules act independently. As shown in Fig. 6, transport takes place in four steps:

a) recombination of an ion and the neutral carrier at the left-hand interface
b) translocation of the complex to the right-hand interface
c) dissociation of the complex and release of the ion into the solution and
d) back transport of the free carrier.

The association with $k^R c_M$ and the dissociation with k^D, as well as the movement of the uncharged carrier, are assumed to be voltage-independent, in contrast to the voltage-dependent rate frequencies k' and k''. We presume a great reservoir of ions in the outer aqueous solution, so that changes in the ion concentration c_M can be neglected.

4.2.1. Voltage-current characteristic. Under non-equilibrium conditions, the current clamp will cause a stationary voltage U_S, if the current I is not too large. The current-voltage characteristic (Fig. 7) has been calculated from phenomenological differential equations (27) and shows saturation behaviour.

$$\frac{d\langle N_1\rangle}{dt} = k^S\langle N_2\rangle + k^D\langle N_3\rangle - (k^R c_M + k^S)\langle N_1\rangle$$

$$\frac{d\langle N_2\rangle}{dt} = k^S\langle N_1\rangle + k^D\langle N_4\rangle - (k^R c_M + k^S)\langle N_2\rangle$$

$$\frac{d\langle N_3\rangle}{dt} = k^R c_M\langle N_1\rangle + k''\langle N_4\rangle - (k^D + k')\langle N_3\rangle$$

$$\frac{d\langle N_4\rangle}{dt} = k^R c_M\langle N_2\rangle + k'\langle N_3\rangle - (k^D + k'')\langle N_4\rangle \qquad (27)$$

As a consequence, the current I may not be selected greater than the upper limit, if a stationary value of the voltage is to be received. Otherwise, there will be an infinite increase in the voltage, because the voltage-independent rate frequencies set a limit to the transport through the membrane. $N_i (i=1, 2, 3, 4)$ denote the occupation numbers of the carriers according to (Fig. 6). The values for the stationary process are indicated with the index *s*. Then

$$I = q(k'_S\langle N_3\rangle_S - k''_S\langle N_4\rangle_S). \qquad (28)$$

The rate frequencies k'_S and k''_S depend on the stationary voltage U_S (4). The mean values of the occupation numbers can be calculated from the stationary solution of (27). Figure 7 shows the dependence of the current and the stationary voltage, which has been calculated with parameters experimentally determined for the carrier valinomycin by Benz and Läuger (1976).

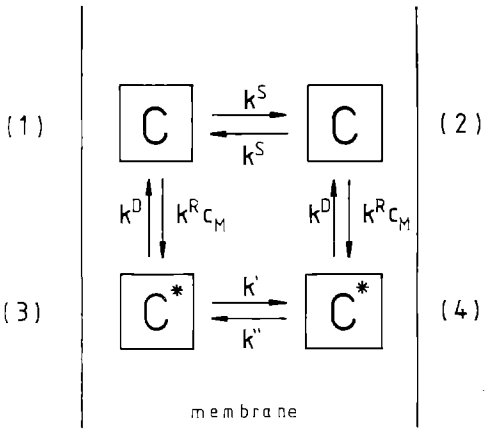

Fig. 6. State diagram for a model of carrier-mediated ion transport. C: uncharged carrier, C^*: charged carrier

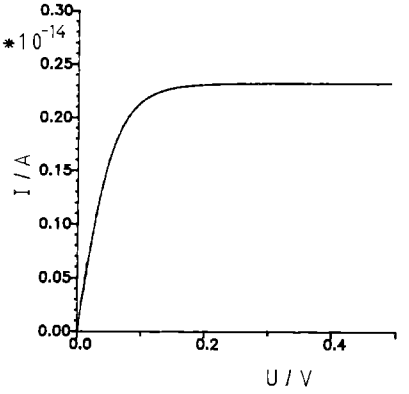

Fig. 7. Current-voltage characteristic for an ion carrier. $k^R c_M = 2.9 \cdot 10^5\ s^{-1}$, $k^D = 2.7 \cdot 10^5\ s^{-1}$, $k^S = 0.38 \cdot 10^5\ s^{-1}$, $k'(0) = k''(0) = 2.1 \cdot 10^5\ s^{-1}$, $N_C = 1$, $k_B = 1.3806 \cdot 10^{-23}$ J/K, $T = 298$ K, $q = 1.6022 \cdot 10^{-19}$ C, (Benz and Läuger 1976)

4.2.2. The time-behaviour of the voltage after a current jump. After a current jump, the voltage will increase from zero to the stationary value U_S if the current does not exceed the upper limit as described above. We will compare the voltage courses, which result from Monte-Carlo-simulations and from the phenomenological differential equations (27). Under non-equilibrium conditions an equation analogous to (28) can be written:

$$I = q(k'\langle N_3\rangle - k''\langle N_4\rangle) + C\frac{d\langle U\rangle}{dt}. \qquad (29)$$

The additional term

$$C\frac{d\langle U\rangle}{dt}$$

denotes the change of capacitance charge. An iterative procedure yields the mean voltage $\langle U\rangle$ as a function of

time at the $j+1$ iteration step with the time interval Δt:

$$\langle U\rangle^{j+1}=\langle U\rangle^{j}+\frac{\Delta t}{C} \cdot(I-q(k'(\langle U\rangle^{j})\langle N_3\rangle^{j+1}-k''(\langle U\rangle^{j})\langle N_4\rangle^{j+1})). \tag{30}$$

The mean states $\langle N_3\rangle$, $\langle N_4\rangle$ depending on the voltage, also have to be calculated iteratively: with the definitions

$$\langle \mathbf{N}\rangle := \begin{bmatrix}\langle N_1\rangle\\ \langle N_2\rangle\\ \langle N_3\rangle\\ \langle N_4\rangle\end{bmatrix}, \quad K^R := k^R c_M$$

and

$$\mathbf{M}(U) := \begin{bmatrix} -(k^S+K^R) & k^S & k^D & 0\\ k^S & -(k^S+K^R) & 0 & k^D\\ K^R & 0 & -(k'(U)+k^D) & k''(U)\\ 0 & K^R & k'(U) & -(k''(U)+k^D)\end{bmatrix} \tag{31}$$

Equation (27) can be written in the form

$$\frac{\mathrm{d}\langle \mathbf{N}\rangle}{\mathrm{d}t}=\mathbf{M}(U)\langle \mathbf{N}\rangle \tag{32}$$

and the following iteration is obtained for the states $\langle \mathbf{N}\rangle$

$$\langle \mathbf{N}\rangle^{j+1}=\mathbf{M}(\langle U\rangle^{j})\langle \mathbf{N}\rangle^{j}\Delta t+\langle \mathbf{N}\rangle^{j}. \tag{33}$$

The two iterations (30) and (33) have to be carried out simultaneously.

Figure 8 a–c shows the time behaviour of the voltage after a current jump. The results of the iteration procedure described are compared with the results of the Monte-Carlo-method in the case of a single carrier. A good agreement of these two methods exists for large capacitances. The differences become greater for smaller capacitances because of the increasing fluctuations. Figure 8 c shows that only the Monte-Carlo-simulations exhibit an oscillatory time behaviour. These oscillations have also been obtained for greater numbers of carriers and for different initial values of the voltage.

This effect can be understood by the fact that at low capacitances one transition of an ion through the membrane causes a great change in voltage. Therefore a small increase of voltage as a consequence of the continuous current clamp can not be compensated by a transition. The oscillation can be understood as a continuous voltage increase between two jumps and the subsequent decrease as a consequence of a transition in the opposite current direction.

For testing this explanation, further simulations with a noisy current clamp (i.e. a charge transport, discrete and Poisson-distributed) were performed. Figure 8 c (3), indeed, shows the disappearance of the oscillations.

The deviation of the simulation from the results of the phenomenological equations does not have biological importance because it occurs only at very low values of capacitance. The specific membrane capacitance

$$C_m=\frac{C}{A} \tag{34}$$

has a value of 1 μFcm^{-2} for biological membranes and the area of a patch-clamp-electrode is approximately $A=1\ \mu\mathrm{m}^2$. Therefore a capacitance $C=10^{-14}$ F is of experimental importance. At this value the time behaviour of the voltage and the spectral density (Fig. 9 a, b) from all calculated simulations indicate very good agreement with the results of the phenomenological equations as well as for low numbers of transport units.

4.3. *The single-file-channel with open-closed-kinetics*

Experimental investigations (Frauenfelder et al. 1979; Karplus and McCammon 1983) showed that channels built from proteins can have different states. Such changes of the conformation (Läuger et al. 1980; Läuger 1987) of a channel have a great influence on the transport rates of ions. Furthermore, nerve excitation processes are generated by the ion channels which may assume different conductivity states. As a simple example we studied one special case with three possible states of the channel as demonstrated in Fig. 10 (Frehland 1979): *1.* open and occupied, *2.* open and unoccupied, *3.* closed and unoccupied. It is assumed that the channel can open and close only in an unoccupied state with voltage-independent frequencies ν and μ. The transitions between states 1 and 2 are assumed to occur according to the model of the single-file-channel with one binding site with voltage-dependent transport rates

$$K_1=k'+k''$$
$$K_2=k^L+k^R. \tag{35}$$

In order to get only a basic fluctuation effect, as a further simplification it is assumed that the open-close transition rates are voltage-independent. Hence, the conformation changes of the channels can be regarded as Poisson-distributed. We carried out Monte-Carlo-simulations with a method analogous to that described above. We studied the time behaviour of the mean voltage after a current jump by Monte-Carlo-simulations and by iterative calculations from the phenomenological equations:

$$\langle U\rangle^{j+1}=\langle U\rangle^{j}+\frac{\Delta t}{C} \cdot(I-q(k^L(\langle U\rangle^{j})\langle N_2\rangle^{j+1}-k''(\langle U\rangle^{j})\langle N_1\rangle^{j+1})). \tag{36}$$

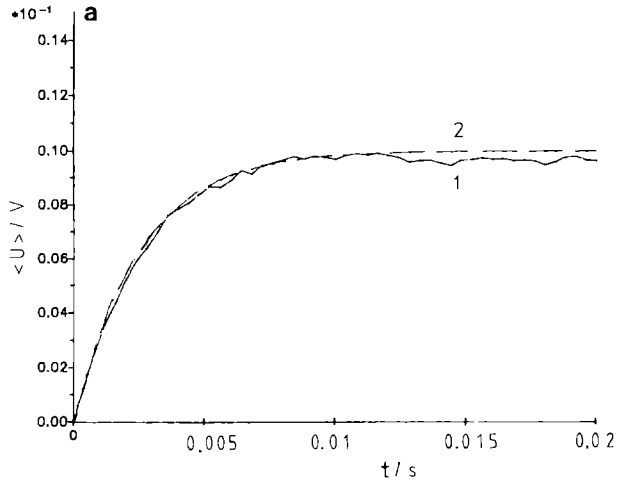

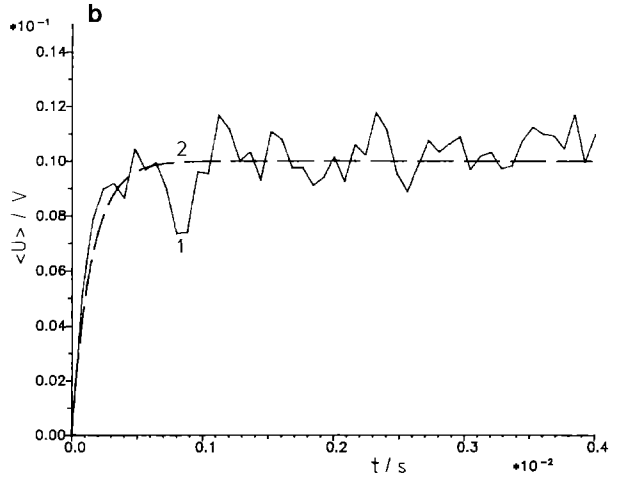

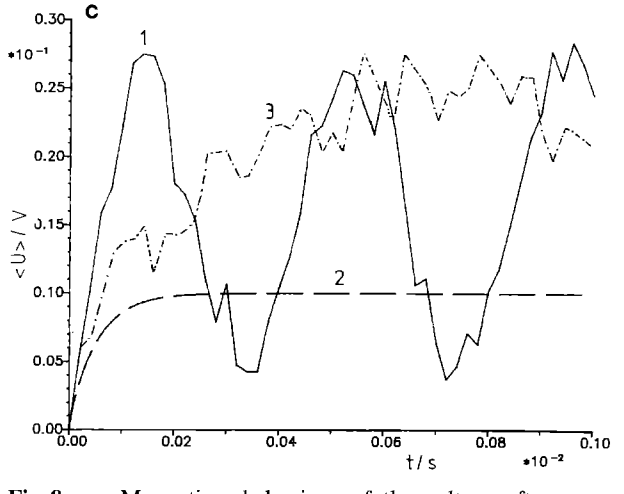

Fig. 8a–c. Mean time behaviour of the voltage after a current jump for an ion carrier. (*1*) Monte-Carlo-simulation, (*2*) (30) and (33). Parameters as in Fig. 7 and: $U_S=10$ mV, **a** $C=10^{-16}$ F, **b** $C=5\cdot10^{-18}$ F, **c** $C=10^{-18}$ F, (*3*): noisy current clamp

$$\langle \mathbf{N}\rangle^{j+1}=\mathbf{M}(\langle U\rangle^j)\,\langle \mathbf{N}\rangle^j\,\Delta t+\langle \mathbf{N}\rangle^j, \tag{37}$$

$$\mathbf{M}(U)=\begin{bmatrix} -K_1(U) & K_2(U) & 0 \\ K_1(U) & -(\mu+K_2(U)) & \nu \\ 0 & \mu & -\nu \end{bmatrix}. \tag{38}$$

A comparison of the results from these two methods is shown in Fig. 11 a, b. The following parameters were used:

N_P, k_B, T, q, k^L, k^R, k', $k''=1$, $\nu=\mu=0.01$, $U_S=5$, $\gamma_{1,2}=0.5$, a: $C=10$, b: $C=100$.

Figure 11 a shows a great difference between the two methods if only one channel exists. The differences become smaller for a greater number of pores as further calculations showed. The phenomenological equations do not take into account the fact that fluctuations can also influence the mean time behaviour. If all pores are closed, the voltage will increase linearly in time because of the current clamp. The voltage can only be reduced if a

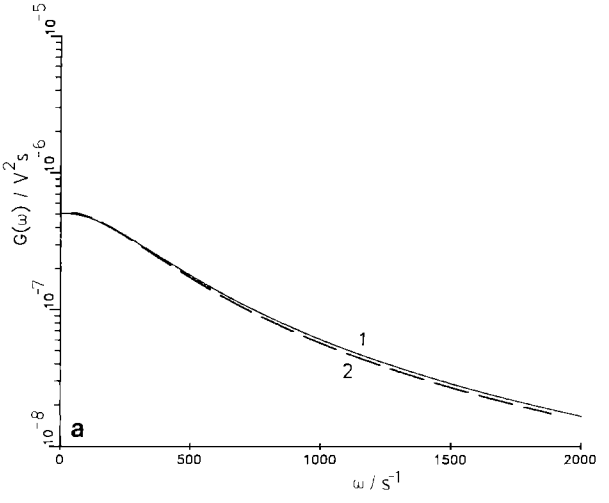

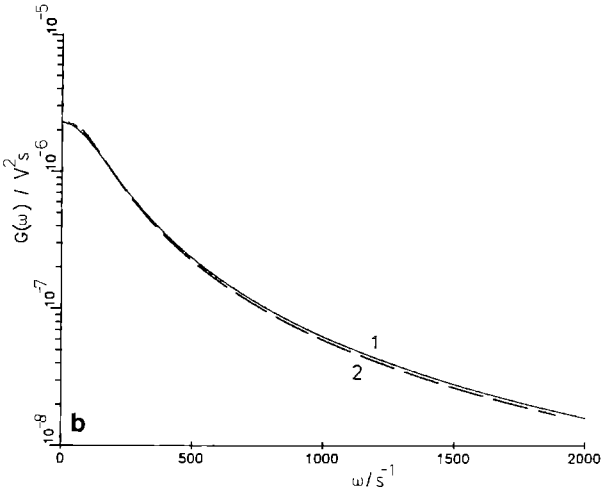

Fig. 9a, b. Spectral density for an ion carrier. (*1*) Monte-Carlo-simulation, (*2*) theory of Frehland and Solleder 1986. Parameters as in Fig. 8 a except: **a** $U_S=20$ mV, **b** $U_S=60$ mV

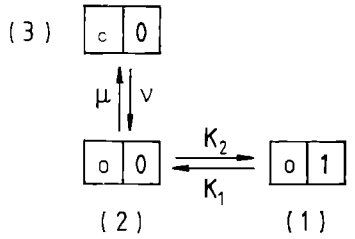

Fig. 10. State diagram for a single-file-channel with open-closed-kinetics: (*1*) Open and occupied, (*2*) open and unoccupied, (*3*) closed and unoccupied

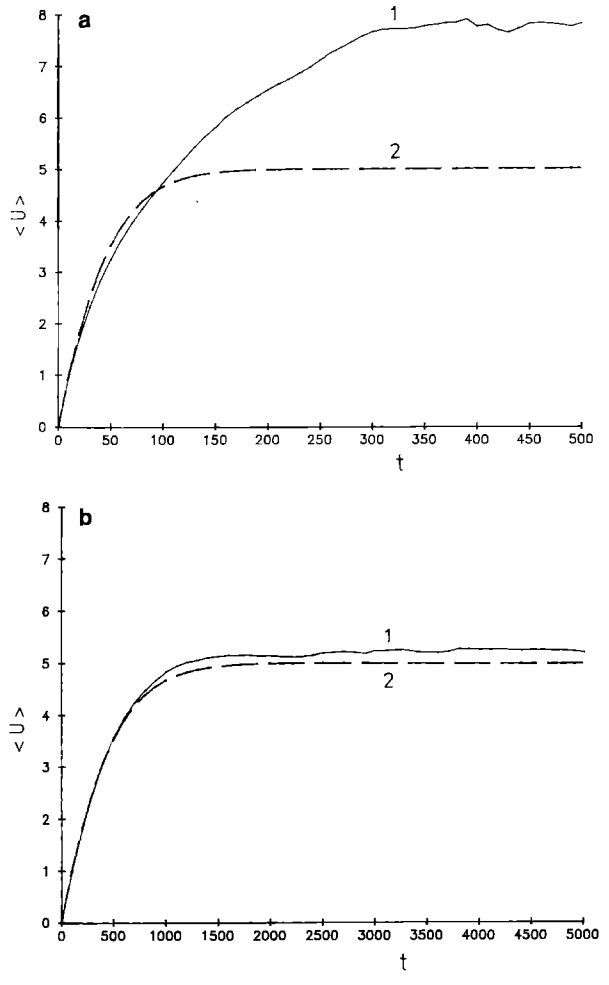

Fig. 11 a, b. Mean time behaviour of the voltage after a current jump for a single-file-channel with open-closed-kinetics. (*1*) Monte-Carlo-simulation, (*2*) (36), (37). N_P, k_B, T, q, $k^L(0)$, $k^R(0)$, $k'(0)$, $k''(0)=1$, $\nu=\mu=0.01$, $\gamma_{1,2}=0.5$, $U_S=5$, **a** $C=10$, **b** $C=100$

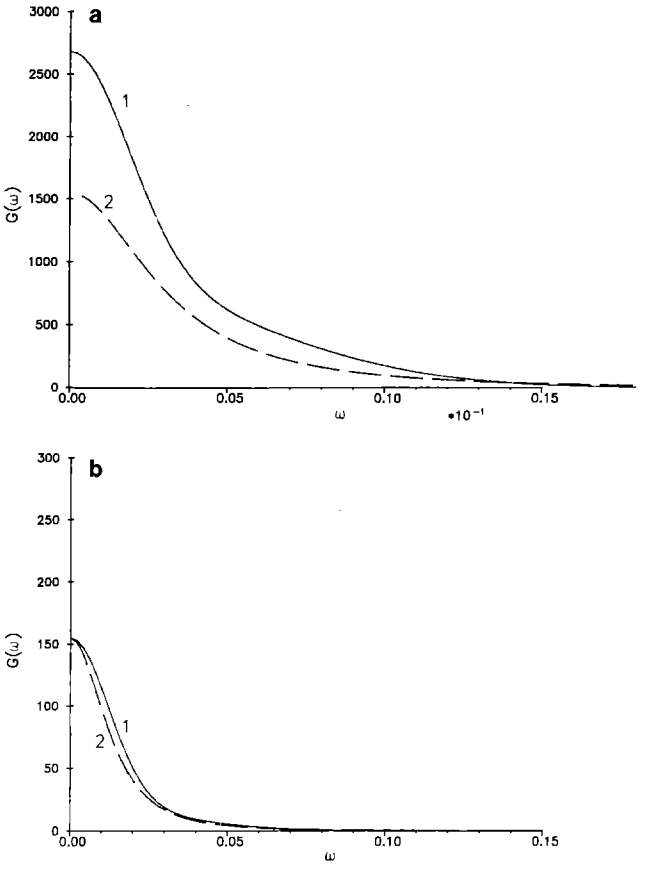

Fig. 12 a, b. Spectral density for a single-file-channel with open-closed-kinetics. (*1*) Monte-Carlo-simulation, (*2*) theory of Solleder and Frehland (1986). Parameters as in Fig. 11 b except: **a** $N_P=1$, **b** $N_P=10$

channel is open. The smaller the number of pores, the greater is the possibility that all pores are in the closed state. Therefore, especially for small numbers of transport units, the voltage can reach values which are much higher than the mean value. So the approach to the results from the phenomenological equations can be understood as a consequence of the negligible fluctuations in the case of large numbers of pores.

As can be seen from Fig. 11 a, b, the deviation of the two methods also depends on the capacitance of the membrane. The effect of the deviation at a capacitance which is a factor of ten greater seems to be negligible if we consider the mean voltage course. However, the spectral density (Fig. 12 a) shows that the condition for linearisation in the previous theory is not valid for small numbers of transport units. For $N_P=10$ (Fig. 12 b) a quite good agreement with the previous theory is already obtained.

Parameters like the Boltzmann constant k_B or the temperature T or the unit charge q were set in our calculations to be equal to unity. A proper scaling of the parameters allows predictions for biologically relevant ranges. Using the method of dimensional analysis (Görtler 1975; Isaacson E. and Isaacson M. 1975; Langhaar 1951; Legendre P. and Legendre L. 1983), the following linear, independent dimensionless products can be determined:

$$\pi_1=\frac{q^2}{2\,k_B\,T\,C} \qquad \pi_2=t\cdot k^i \quad \text{with} \quad i=L,R,',''$$

$$\pi_3=t\cdot\mu \qquad \pi_4=t\cdot\nu$$

$$\pi_5=\frac{U\,C}{q} \qquad \pi_6=\frac{I}{q\,k^i}$$

$$\pi_7=\frac{C(s)\,C^2}{q^2} \qquad \pi_8=\frac{G(f)\,C^2\,k^i}{q^2}. \tag{39}$$

Each set of parameters with the same dimensionless products is given by a single calculation. For instance, the simulation in Fig. 12 yields

$$\pi_1 = 0.005.$$

If experimentally relevant parameters are considered, with $k_B = 1.3806 \cdot 10^{-23}$ J/K, $T = 298$ K, $q = 1.6022 \cdot 10^{-19}$ C, the capacitance will have the value

$$C = \frac{q^2}{2 k_B T \pi_1} = 0.62 \cdot 10^{-15} \text{ F}.$$

This value is about one order of magnitude less than the capacitance of a piece of a membrane under a patch-clamp-pipette. Scaling of other parameters (e.g. of the spectral density) can be done analogously. As a consequence of the too small capacitance, this calculation yields fluctuations which will be greater than in the experimental system. However, the ratios of the inner transition rates k^i to the frequencies ν, μ of the opening and closing of the channel essentially determine the magnitude of the fluctuations. In Fig. 12 the value for this ratio is $1/0.01 = 100$. But experimental investigations showed that this ratio can be $10^8/10^3 = 10^5$.

In order to have an acceptable computer-calculating-time, we chose the ratio $1/0.01 = 100$. On the one hand, the selected capacitance leads to an overestimate of the fluctuations; on the other hand, the time ratio yields a much greater underestimate of the fluctuations. The reason is, that in experiments, pores can remain in a closed state for a very long time in proportion to the inner mean transition time. During this period, the voltage will increase enormously if all pores are closed. Therefore we predict that in experimentally relevant ranges of parameters, the previous theory will no longer be applicable if only a small number of transport units is considered.

Acknowledgement. This work has been financially supported by the Deutsche Forschungsgemeinschaft.

References

Bendat JS, Piersol AG (1971) Random data: analysis and measurement procedures. Wiley, New York

Benz R, Läuger P (1976) Kinetic analysis of carrier-mediated ion transport by the charge-pulse technique. J Membrane Biol 27:171–191

DeFelice LJ (1981) Introduction to membrane noise. Plenum Press, New York

Dubin N (1976) A stochastic model for immunological feedback in carcinogenesis. Lecture Notes in Biomathematics, vol 9. Springer, Berlin Heidelberg New York

Eyring H (1935) The activated complex in chemical reactions. J Chem Phys 3:107–115

Frauenfelder H, Petsko GA, Tsernoglu D (1979) Dynamics of proteins: elements and function. Nature 280:558–563

Frehland E (1978) Current noise around steady states in discrete transport systems. Biophys Chem 8:255–265

Frehland E (1979) Theory of transport noise in membrane channels with open-closed kinetics. Biophys Struct Mechanism 5:91–106

Frehland E (1982) Stochastic transport processes in discrete biological systems. Lecture Notes in Biomathematics, vol 47. Springer, Berlin Heidelberg New York

Frehland E (1988) Stochastic analysis of discrete markovian systems. 1. Steady state fluctuations of scalar and vectorial quantities. J Non-Equilib Thermodyn 13:133–146

Frehland E, Solleder P (1985) Non-equilibrium voltage noise generated by ion transport through pores. Eur Biophys J 11:167–178

Frehland E, Solleder P (1986) Nonequilibrium voltage fluctuations in biological membranes. 1. General framework of charge transport in discrete and related voltage noise. Biophys Chem 25:135–145

Frehland E, Stephan W (1979) Theory of single-file noise. Biochim Biophys Acta 553:326–341

Görtler H (1975) Dimensionsanalyse: Theorie der physikalischen Dimensionen mit Anwendungen. Springer, Berlin Heidelberg New York

Isaacson E de St Q, Isaacson M de St Q (1975) Dimensional methods in engineering and physics. Edward Arnold, London

Karplus M, McCammon JA (1983) Temperature-dependent X-ray diffraction as a probe of protein structural dynamics. Ann Rev Biochem 52:263–300

Khintchine A (1934) Korrelationstheorie der stationären stochastischen Prozesse. Math Ann 109:604–615

Kirkpatrick S, Stoll EP (1981) A very fast shift-register sequence random number generator. J Comp Phys 40:517–526

Kleutsch B (1988) Monte-Carlo-Simulationen stochastischer Transportprozesse unterschiedlicher Dimensionalität in biologischen Systemen. (Thesis), Hartung-Gorre, Konstanz

Knoll W, Stark G (1975) An extend kinetic of valinomycin-induced Rb-transport through monoglyceride membranes. J Membrane Biol 25:249–270

Langhaar HL (1951) Dimensional analysis and theory of models. Wiley, New York

Läuger P (1975) Shot noise in ion channels. Biochim Biophys Acta 413:1–10

Läuger P (1987) Ion movement through channels with conformational substates. Ion Transport through Membranes: 85–99

Läuger P, Stark G (1970) Kinetics of carrier-mediated ion transport across lipid bilayer membranes. Biochim Biophys Acta 211: 458–466

Läuger P, Stephan W, Frehland E (1980) Fluctuations of barrier structure in ionic channels. Biochim Biophys Acta 602:167–180

Legendre P, Legendre L (1983) Numerical ecology. Elsevier/North Holland, New York Amsterdam

Sobol IM (1971) Die Monte-Carlo-Methode. Deutscher Verlag der Wissenschaften, Berlin

Solleder P, Frehland E (1986) Nonequilibrium voltage fluctuations in biological membranes. 2. Voltage and current noise generated by ion carriers, channels and electrogenic pumps. Biophys Chem 25:147–159

Stark G, Ketterer B, Benz R, Läuger P (1971) The rate constants of valinomycin-mediated ion transport through thin lipid membranes. Biophys J 11:981–994

Vliet KM van, Fassett JR (1965) Fluctuations due to electronic transitions and transport in solids. In: Burges RE (ed) Fluctuation phenomena in solids. Academic Press, New York, pp 267–354

Wiener N (1930) Generalized harmonic analysis. Acta Math 55: 117–258

Zwolinski BJ, Eyring H, Reese CE (1949) Diffusion and membrane permeability. J Phys Chem 53:1426–1453